PROCEEDINGS OF SCIENCE

Photon pair production: full NNLO corrections in QCD with heavy quark mass dependence

Federico Coro[a,*]

[a] *Instituto de Fisica Corpuscolar, Universitat de Valencia - Consejo Superior de Investigaciones Cientificas, Parc Cientific, E-46980 Paterna, Valencia, Spain*

E-mail: fcoro@ific.uv.es

We consider the photon pair production at the next-to-next-to-leading order (NNLO) in perturbative QCD at the LHC, taking into account for the first time the full top quark mass dependence. We present the computation of the two-loop form factors for diphoton production in the quark annihilation channel. We discuss the relevant scalar integral families for the process and the master integrals (MIs) are evaluated by means of differential equations. Finally, we discuss the phenomenological results showing the relevant ratios of the fully massive computation with respect to the massless ones.

Loops and Legs in Quantum Field Theory (LL2024)
14-19, April, 2024
Wittenberg, Germany

*Speaker

PoS(LL2024)041

1. Introduction

The production of two prompt photons is one of the most important processes at the LHC for several reasons. Due to the clear signature of the photons in the LHC calorimeters, diphoton production is important for measuring the fundamental parameters within the Standard Model and at the same time for searching for new physics. For the same reason, it was one of the two most important channels for the discovery of the Higgs boson, and it still constitutes an irreducible QCD background for the Higgs.
The state of the art for this process included scattering amplitudes in the massless case up to NNLO [1–4] and in the massive case the $gg \to \gamma\gamma$ with partial N^3LO contributions [5–8]. Furthermore, amplitudes for $\gamma\gamma + j$ [9–13] and form factors up to 3 loops in the massless case [14] have been known in literature. For a full NNLO accuracy, there was still one contribution missing. We discuss the computation of our main contribution, i.e. the two-loop massive form factors for the partonic process $q\overline{q} \to \gamma\gamma$ [15] and then we use this result in order to consider for the first time diphoton production at NNLO, taking into account the full top quark mass dependence [16], including all the massive contributions.

2. Two-Loop form factors in the quark annihilation channel

In this section we consider the computation of the two-loop form factors in the quark annihilation channel with a heavy quark running in the loop. This was the last missing ingredient for a full NNLO study of the diphoton production in QCD.
At the partonic level, the scattering amplitude is represented by:

$$q(p_1) + \overline{q}(p_2) = \gamma(p_3) + \gamma(p_4), \tag{1}$$

where the external particles are on-shell, i. e. $p_i^2 = 0$.
Using tensor decomposition [17], our amplitude can be decomposed as:

$$\mathcal{A}_{q\overline{q},\gamma\gamma}(s,t,m_t^2) = \sum_{i=1}^{4} \mathcal{F}_i(s,t,m_t^2) T_i, \tag{2}$$

where the F_i are the scalar form factors and the $T_i = \overline{v}(p_2)\Gamma_i^{\mu\nu}u(p_1)\epsilon_{3,\mu}\epsilon_{4,\nu}$ are the independent Lorentz tensors, which depends only on the external momenta and polarisations. We choose the tensors as:

$$\Gamma_1^{\mu\nu} = \gamma^\mu p_2^\nu, \quad \Gamma_2^{\mu\nu} = \gamma^\nu p_1^\mu, \quad \Gamma_3^{\mu\nu} = p_{3,\rho}\gamma^\rho p_1^\mu p_2^\nu, \quad \Gamma_4^{\mu\nu} = p_{3,\rho}\gamma^\rho g^{\mu\nu}. \tag{3}$$

The form factors admits a perturbative expansion in the strong coupling and since we are interested in computing the massive corrections that starts to appear at $O(\alpha_s^2)$, we just need to study this part of the expansion:

$$\mathcal{F}_k^{(2)} = \delta_{ij} C_F (4\pi\alpha_{em}) \left[Q_q^2 \mathcal{F}_{k,top;0}^{(2)} + Q_t^2 \mathcal{F}_{k,top;2}^{(2)} \right], \tag{4}$$

where Q_q is the charge of the light quark, Q_t is the charge of the heavy quark, δ_{ij} is the Kronecker delta on the colors of the incoming quarks and C_F is the Casimir of the fundamental representation of $SU(N_c)$.

Our form factors do not have IR poles, they only have UV poles coming from the term proportional to $\mathcal{F}^{(2)}_{k,top;0}$. They are renormalized adopting a mixed renormalization scheme in which the external quark fields are renormalized on-shell, while α_s is renormalized such that the contribution coming from the light-quarks is in $\overline{MS}$ and the contribution from the heavy-quark is on-shell.

We generated the Feynman diagrams with QGRAF [18] and FeynArts [19] . In Fig. 1, we show a representative subset of them.

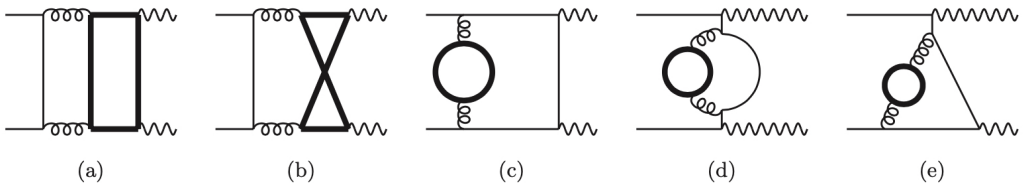

Figure 1: Representative set of two-loop diagrams with internal heavy-quark loops, which contribute at NNLO QCD to diphoton production in the quark annihilation channel. Thin black lines represents light quarks, thick black lines heavy quarks, curly lines gluons and wavey lines photons.

We have identified two planar topologies, PLA and PLB, and a non-planar topology NPL.

The form factors are expressed in terms of a basis of MIs, exploiting IBPs reductions. Identifying all the common MIs, we have built our amplitude in terms of only 42 MIs (modulo permutation of the external legs).

The MIs for the PLA and PLB families were already studied [20]. We presented, as original result, a new set of MIs coming from the NPL, represented in Fig. 2

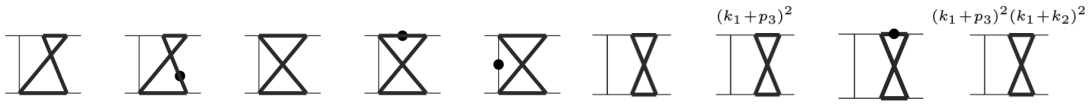

Figure 2: New set of MIs coming from the NPL integral family

The MIs are evaluated through the differential equations method. Specifically, we studied the three topoplogies separately. For the PLA family, we put the system of differential equations, with respect to the kinematics invariants $\underline{x} = \{y, z\}$, where $y = \frac{s}{m_t^2}$ and $z = \frac{t}{m_t^2}$, in canonical logarithmic form [21] . The vector of boundary conditions is $\underline{x} = 0$, where all except two MIs vanishes. In principle, given the system in canonical logarithmic form with the set of d-log forms it would be possible to find an analytic solution for the MIs. However, there is a set of 5 non simultaneously rationalizable square roots and the solution is non trivial. Furthermore, since we were interested in phenomenological study, we decided to not provide an analytical solution, and the MIs were evaluated semi-analytically exploiting the generalised power series expansion method [22], implemented in DiffExp [23].

For the PLB family all the MIs, except one, are equal to one of the MIs of the other two families. The last MIs were already know and his analytic solution was already provided.

Fot the NPL family, the situation was more complicated. We wrote the system of DEs in the following form:

$$d\underline{g}(\underline{x},\epsilon) = \epsilon dA(\underline{x})\underline{g}(\underline{x},\epsilon) + d\tilde{A}(\underline{x},\epsilon)\underline{g}(\underline{x},\epsilon). \tag{5}$$

This means that the system is divided into two different subsets. The first one is given by the MIs whose differential equations can be putted in canonical logarithmic form, while the second is given by MIs whose analytic structures involves integration over elliptic kernels [24, 25]. For the first subset the situation is also more complicated than PLA, since we have here 9 non simultaneously rationalizable square roots. The second subset has two elliptic sectors: the first one is given by the non-planar triangle and the second by our new double-box top sector.

We have studied the homogeneous system of differential equations through the maximal cut in Baikov representation:

$$MC\Big(\quad\Big) \propto \int \frac{dz}{\sqrt{(z+t)(s+t+z)((z+t)(s+t+z)-4sm_t^2)}}, \tag{6}$$

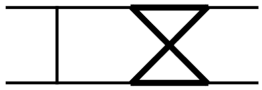

and, as expected, we got an elliptic curve.

We observed that with a Möbius transformation, $z \to z - t$, the elliptic curve is the same obtained for the non-planar triangle [26]. New studies have been done to determine an epsilon-factorized form on the maximal cut [27].

Since we were interested in phenomenological studies, we decided to solve the MIs semi-analitically through the generalised power series technique. This has several advantages, first of all, it doesn't depend on the function space, so we can completely avoid elliptic integrals and, most importantly, we can evaluate the MIs at arbitrary phase-space points with arbitrary precision.

At NNLO, the cross-section for this process can be computed in the q_T-subtraction scheme [28]:

$$d\sigma^{\gamma\gamma}_{NNLO} = \mathcal{H}^{\gamma\gamma}_{NNLO} \otimes d\sigma^{\gamma\gamma}_{LO} + [d\sigma^{\gamma\gamma+j}_{NLO} - d\sigma^{CT}_{NLO}], \tag{7}$$

where the terms inside the square brackets represent the cross section for diphoton plus jet production at NLO and the corresponding counterterm needed to cancel the singularities for small q_T. Our massive corrections are inside the $\mathcal{H}^{\gamma\gamma}_{NNLO}$ term. Specifically:

$$\mathcal{H}^{\gamma\gamma} = \frac{|\mathcal{A}^{(fin)}_{q\bar{q},\gamma\gamma}|^2}{|\mathcal{A}^{(0)}_{q\bar{q},\gamma\gamma}|^2}. \tag{8}$$

We made a grid for the hard function covering the $2 \to 2$ physical space:

$$s > 0, \quad t = -\frac{s}{2}(1 - cos\theta), \quad -s < t < 0, \tag{9}$$

where θ is the scattering angle in the partonic center of mass frame.

The grid in Fig. 3 was prepared for a total of 13752 phase-space points, in the range:

$$-0.99 < \cos\theta < 0.99, \quad 8\,\text{GeV} < \sqrt{s} < 2.2\,\text{TeV}\,. \tag{10}$$

The evaluation times for the different topologies, on a single CPU core, are of $O(2.5h)$ for PLA and $O(10.5h)$ for NPL.

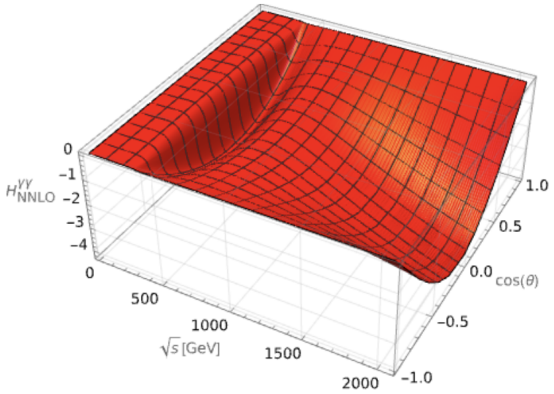

Figure 3: Numerical grid for $\mathcal{H}^{\gamma\gamma}_{\mathrm{NNLO}}$ as function of $\sqrt{s}$ and $cos(\theta)$

The grid for phenomenology was interpolated with cubic spline interpolation. In particular, to check the results, a second grid was prepared in some points evaluated with the interpolation method and the check was made computing the percentage error:

$$\%\ Error = \frac{\mathcal{H}^{\gamma\gamma}_{NNLO-grid}(p_{i,j}) - \mathcal{H}^{\gamma\gamma}_{NNLO-spline}(p_{i,j})}{\mathcal{H}^{\gamma\gamma}_{NNLO-grid}(p_{i,j})} \sim \mathcal{O}(0.3\%) \tag{11}$$

In Fig. 4 we show the points, corresponding to the evaluation of the first grid, in red, and the petrol colored point for the evaluation of the second grid.

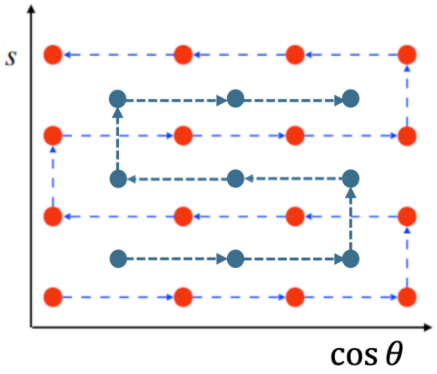

Figure 4: Schematic representation of the procedure exploited to build the two grids with DiffExp. The dots represents the points in which the MIs are evaluated and the dashed lined connect two sequential evaluations.

3. NNLO results with full top-quark mass dependence

In this section we include our scattering amplitude with the previously known massive and massless amplitudes in order to present our results about the full NNLO QCD corrections to diphoton productions. We studied isolated diphoton production in pp collisions at the center-of-mass energy $\sqrt{s} = 13\ TeV$ and we fixed the top quark mass to $m_t = 173\ GeV$. We decided to adopt the smooth

cone isolation criterion [29, 30] in order to avoid possible fragmentation components and possible quark-photon collinear divergences. In particular we fixed the size R of the cone around the photon to allow only the hadronic activity, inside the cone, that satisfy:

$$E_T^{had}(r) \leq \epsilon p_{T_\gamma} \chi(r; R), \tag{12}$$

where p_{T_γ} is the transverse momentum of the photon and $\chi(r; R)$ is a smooth function that goes to zero for $r \to 0$. We used the fiducial cuts discussed in the ATLAS Collaboration study in [31].
The central factorization and renormalization scale is chosen to be equal to the invariant mass of the diphoton pair $\mu \equiv \mu_R = \mu_F = M_{\gamma\gamma}$ and the theoretical uncertainty is estimated by a seven-point scale variation.

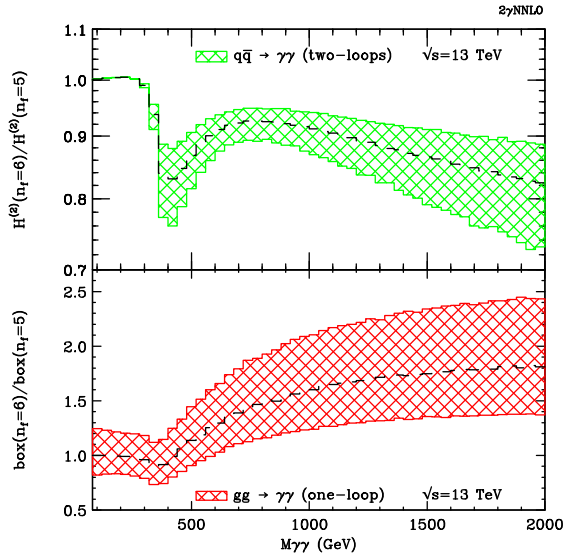

Figure 5: Ratio of different massive corrections to the massless one. In the upper panel the ratio for the 2-loop $q\bar{q}$-channel and in the lower panel the ratio for the 1-loop box in the gg-channel.

In the upper panel of Fig. 5 we show the ratio between the fully massive and the massless invariant mass distribution of the two-loop hard function. As expected the distribution exhibits its negative peak around the top-quark pair threshold ($2m_t$). After a second peak around $2.3 \cdot 2m_t$ the tail decreases. We observe that also the correction obtained considering six light quark flavors is smaller than the corresponding one with five flavors. In the bottom panel we show the ratio of the one-loop box in the gg-channel. We have the negative peak around the top-quark pair threshold, but contrary to what happens in the $q\bar{q}$ case, here the tail is not decreasing . Furthermore, asymptotically ($M_{\gamma\gamma} >> m_t$) the ratio approaches to $\frac{(\sum_{n_f} e_q^2)^2}{(\sum_{n_f=5} e_q^2)^2} = \frac{225}{121}$, implying that the massive contribution behaves as if it were composed by six light quark flavors.
In Fig. 6 we present our final result about the invariant mass distribution of the diphoton at NNLO in perturbative QCD. In the lower panel we show the ratio between the fully massive NNLO result and the NNLO prediction for five light quark flavors. We have the negative peak around the top-quark pair threshold due to a superposition of the effects from the different loop contributions. For $M_{\gamma\gamma} > 2m_t$ we have a positive peak around $2 \cdot 2m_t$ and subsequently the massive corrections

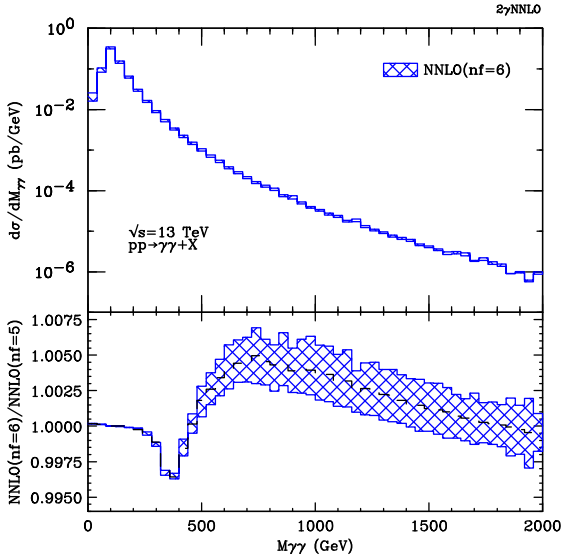

Figure 6: NNLO invariant mass distribution with full top quark mass dependence.

becomes larger than the massless one. Specifically, in the invariant mass region 1 $GeV < M_{\gamma\gamma} < 2$ TeV the deviation from the massless result is in the range $[-0.4\%, 0.8\%]$.
We want to underline that due to the vanishing luminosity of the gluons for large values of $M_{\gamma\gamma}$, our corrections in the $q\overline{q}$-channel will be dominant in the high invariant mass region.

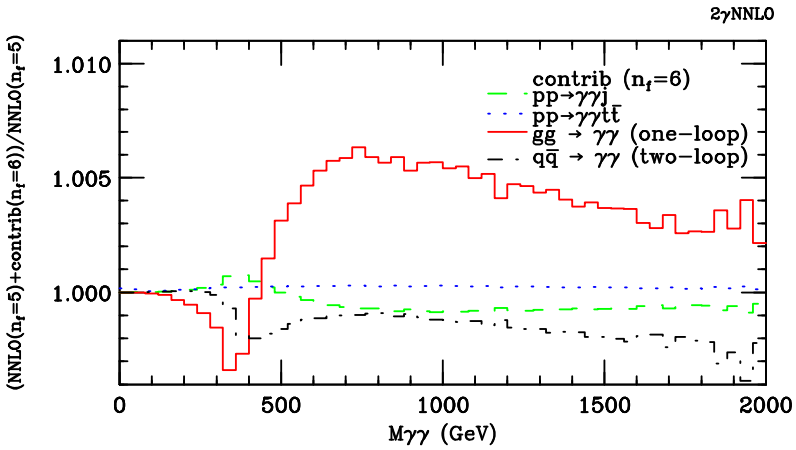

Figure 7: Ratios of each massive contribution with respect to the NNLO massless cross section as a function of the invariant mass.

Finally, in Fig. 7 we show the ratio of each massive contribution to the diphoton production up to NNLO. In particular we have the two-loop (double-virtual) corrections to the Born sub-process $q\bar{q}$, the real radiation contributions (real-virtual and double-real) and the box in gluon fusion. As expected, at this order, the $q\overline{q}$ (dot-dashed black line) and the gg one-loop box (red line) are the most sizeable contributions in the full invariant mass range. The double-real corrections (dotted blue line) are not relevant for phenomenology and since they are due to the tree-level production of

on-shell top quarks there is no peak around the threshold. The effect of the real-virtual corrections (dashed green line) reduces the size of the negative peak around the top-quark pair threshold, but it is subdominant with respect to the other corrections.

4. Conclusions

We presented the computation of the last missing part for a full study of diphoton production at NNLO in QCD. In particular, we discussed the computation of the two-loop form factors and the relevant scalar integral families in the quark-annihilation channel. We showed that some of the new MIs of the NPL family are related to a genus one Riemann surface, and we made the connection with the elliptic curve of the non-planar triangle explicit. The MIs were evaluated through the generalized power series technique, and we created a grid in the physical phase-space to perform the phenomenology. Finally, we show the invariant mass distribution of the full NNLO diphoton production in QCD and the relevant ratios of the fully massive contributions with respect to the massless ones.

Acknowledgements

This work is supported by the Spanish Government (Agencia Estatal de Investigación MCIN/AEI/10.13039/501100011033) Grant No. PID2020-114473GB-I00, and Generalitat Valenciana Grants No. PROMETEO/2021/071 and ASFAE/2022/009 (Planes Complementarios de I+D+i, Next Generation EU). F.C. is supported by Generalitat Valenciana GenT Excellence Programme (CIDEGENT/2020/011) and ILINK22045.

References

[1] Stefano Catani, Leandro Cieri, Daniel de Florian, Giancarlo Ferrera, and Massimiliano Grazzini. Diphoton production at the LHC: a QCD study up to NNLO. *JHEP*, 04:142, 2018.

[2] John M. Campbell, R. Keith Ellis, Ye Li, and Ciaran Williams. Predictions for diphoton production at the LHC through NNLO in QCD. *JHEP*, 07:148, 2016.

[3] R. Schuermann, X. Chen, T. Gehrmann, E. W. N. Glover, M. Höfer and A. Huss, *NNLO Photon Production with Realistic Photon Isolation*, *PoS* **LL2022** (2022) 034, [2208.02669].

[4] S. Catani, L. Cieri, D. de Florian, G. Ferrera and M. Grazzini, *Diphoton production at hadron colliders: a fully-differential QCD calculation at NNLO*, *Phys. Rev. Lett.* **108** (2012) 072001, [1110.2375].

[5] Z. Bern, A. De Freitas and L. J. Dixon, *Two loop amplitudes for gluon fusion into two photons*, *JHEP* **09** (2001) 037, [hep-ph/0109078].

[6] F. Maltoni, M. K. Mandal and X. Zhao, *Top-quark effects in diphoton production through gluon fusion at next-to-leading order in QCD*, *Phys. Rev. D* **100** (2019) 071501, [1812.08703].

[7] Z. Bern, L. J. Dixon and C. Schmidt, Phys. Rev. D **66** (2002), 074018 doi:10.1103/PhysRevD.66.074018 [arXiv:hep-ph/0206194 [hep-ph]].

[8] L. Chen, G. Heinrich, S. Jahn, S. P. Jones, M. Kerner, J. Schlenk, H. Yokoya, Photon pair production in gluon fusion: Top quark effects at NLO with threshold matching, JHEP 04 (2020) 115. arXiv:1911.09314, doi:10.1007/JHEP04(2020)115.

[9] H. A. Chawdhry, M. Czakon, A. Mitov and R. Poncelet, *Two-loop leading-colour QCD helicity amplitudes for two-photon plus jet production at the LHC*, *JHEP* **07** (2021) 164, [2103.04319].

[10] B. Agarwal, F. Buccioni, A. von Manteuffel and L. Tancredi, *Two-Loop Helicity Amplitudes for Diphoton Plus Jet Production in Full Color*, *Phys. Rev. Lett.* **127** (2021) 262001, [2105.04585].

[11] H. A. Chawdhry, M. Czakon, A. Mitov and R. Poncelet, *NNLO QCD corrections to diphoton production with an additional jet at the LHC*, *JHEP* **09** (2021) 093, [2105.06940].

[12] S. Badger, T. Gehrmann, M. Marcoli and R. Moodie, Phys. Lett. B **824** (2022), 136802 doi:10.1016/j.physletb.2021.136802 [arXiv:2109.12003 [hep-ph]].

[13] S. Badger, H. B. Hartanto, J. Kryś and S. Zoia, JHEP **11** (2021), 012 doi:10.1007/JHEP11(2021)012 [arXiv:2107.14733 [hep-ph]].

[14] F. Caola, A. Von Manteuffel and L. Tancredi, Phys. Rev. Lett. **126** (2021) no.11, 112004 doi:10.1103/PhysRevLett.126.112004 [arXiv:2011.13946 [hep-ph]].

[15] M. Becchetti, R. Bonciani, L. Cieri, F. Coro, F. Ripani, Two-loop form factors for diphoton production in quark annihilation channel with heavy quark mass dependence (8 2023). arXiv:2308.11412.

[16] M. Becchetti, R. Bonciani, L. Cieri, F. Coro and F. Ripani, *Full top-quark mass dependence in diphoton production at NNLO in QCD*, 2308.10885.

[17] T. Peraro and L. Tancredi, *Tensor decomposition for bosonic and fermionic scattering amplitudes*, *Phys. Rev. D* **103** (2021) 054042, [2012.00820].

[18] P. Nogueira, J. Comput. Phys. **105** (1993), 279-289 doi:10.1006/jcph.1993.1074

[19] T. Hahn, *Generating Feynman diagrams and amplitudes with FeynArts 3*, *Comput. Phys. Commun.* **140** (2001) 418–431, [hep-ph/0012260].

[20] M. Becchetti and R. Bonciani, *Two-Loop Master Integrals for the Planar QCD Massive Corrections to Di-photon and Di-jet Hadro-production*, *JHEP* **01** (2018) 048, [1712.02537].

[21] J. M. Henn, Phys. Rev. Lett. **110** (2013), 251601 doi:10.1103/PhysRevLett.110.251601 [arXiv:1304.1806 [hep-th]].

[22] F. Moriello, *Generalised power series expansions for the elliptic planar families of Higgs + jet production at two loops*, *JHEP* **01** (2020) 150, [1907.13234].

[23] M. Hidding, *DiffExp, a Mathematica package for computing Feynman integrals in terms of one-dimensional series expansions*, *Comput. Phys. Commun.* **269** (2021) 108125, [2006.05510].

[24] F. C. S. Brown and A. Levin, *Multiple elliptic polylogarithms*, 2013.

[25] J. Broedel, C. Duhr, F. Dulat, B. Penante and L. Tancredi, *Elliptic polylogarithms and Feynman parameter integrals*, *JHEP* **05** (2019) 120, [1902.09971].

[26] A. von Manteuffel and L. Tancredi, *A non-planar two-loop three-point function beyond multiple polylogarithms*, *JHEP* **06** (2017) 127, [1701.05905].

[27] T. Ahmed, E. Chaubey, M. Kaur and S. Maggio, JHEP **05** (2024), 064 doi:10.1007/JHEP05(2024)064 [arXiv:2402.07311 [hep-th]].

[28] Stefano Catani, Leandro Cieri, Daniel de Florian, Giancarlo Ferrera, and Massimiliano Grazzini. Universality of transverse-momentum resummation and hard factors at the NNLO. *Nucl. Phys. B*, 881:414–443, 2014.

[29] Stefano Frixione. Isolated photons in perturbative QCD. *Phys. Lett. B*, 429:369–374, 1998.

[30] Stefano Frixione and Werner Vogelsang. Isolated photon production in polarized pp collisions. *Nucl. Phys. B*, 568:60–92, 2000.

[31] ATLAS collaboration, G. Aad et al., *Measurement of the production cross section of pairs of isolated photons in pp collisions at 13 TeV with the ATLAS detector*, *JHEP* **11** (2021) 169, [2107.09330].